ACTA FACULTATIS XYLOLOGIAE ZVOLEN, 67(1): 109−124, 2025
Zvolen, Technická univerzita vo Zvolene
DOI: 10.17423/afx.2025.67.1.10

FOUNDATION OF TIMBER STRUCTURES – CRAWL SPACE HEAT AND MOISTURE ANALYSIS WITH AIR AGE SIMULATION AND OCCURRENCE OF MICROMYCETES

Slávka Pobucká – Pavel Kučírek – Karel Šuhajda – Jan Holešovský

ABSTRACT

This study is focused on the analysis of the crawl space microclimate in timber structures in the Czech Republic. It focused on the conditions in which the timber and fiberboard elements of the crawl space ceiling structure are located. As part of the analysis, air temperature, relative humidity, air flow within the crawl space were monitored. The average relative humidity within the crawl space reached up to 85% in summer and up to 90% in winter. The residence time of air in the crawl space was determined using air age simulation. A long residence time of air in the crawl space may pose a risk of capturing mold spores on the crawl space wall and ceiling surfaces. OpenFOAM software was used for the simulations. The analysis revealed the presence of fungal spores of the genera *Penicillium*, *Aspergillus*, and *Cladosporium.*

Keywords: timber structure; crawl space; micromycetes; age of the air; openFOAM.

INTRODUCTION

A crawl space is a type of building foundation prevalent in regions such as the United States and northern European countries. For instance, up to 56% of detached houses built in Sweden between 1990 and 2003 feature crawl space foundations (Burke, 2007; Lynn *et al*., 2011). There is no tradition of crawl spaces in the Czech Republic, but we have been encountering them more and more often recently. Numerous studies on crawl space microclimates originate from countries where crawl spaces are traditional. These include studies from Finland (Kurnitski and Matilainen, 2000; Matilainen and Kurnitski, 2003; Airaksinen *et al*., 2003; Laukkarinen and Vinha, 2017), Sweden (Bok *et al*., 2009; Airaksinen *et al*., 2020; Risberg and Westerlund, 2020), Denmark (Vanhoutteghem *et al*., 2017) and USA (Erickson and Zhai, 2008). These studies focus not only on monitoring the temperature and relative humidity in the crawl space but also on the possibility of ventilation in the space or the occurrence of mold on the structure's surfaces. Investigations of numerical simulations in the crawl space were also conducted with the aim of predicting the temperature and humidity conditions within the crawl space (Vanhoutteghem *et al*., 2017).

Generally, the most significant problem related to crawl spaces is high relative humidity, which can reach values up to 85% - 95%. During the summer months, water vapor can condense on the cooler surface of the structure (Kurnitski and Matilainen, 2000; Matilainen and Kurnitski, 2003). The ceiling structure or foundation walls can be damaged by persistent high humidity in the crawl space. The ceiling structure is usually made of wood and wood-fiber material. The wooden element in the crawl space is the foundation sill of the load-bearing walls of the first floor. It can also cause deterioration of indoor air quality and may be associated with health problems. The repair needs of buildings damaged by dampness and mold are addressed in a study (Annila *et al*., 2018), which found that up to 85% of the surveyed crawl space buildings required repair. A study from China and Japan (Yuan *et al*., 2024) highlighted the problem of high humidity in buildings with walls in contact with the ground. A crawl space can also be considered a type of structure. The thermal capacity of the ground contributes to lower temperatures during spring and summer, as well as higher relative humidity. The evaporation of soil moisture from the bottom of the crawl space can be influenced by the type of covering of the crawl space itself and the intensity of air exchange in the space (Airaksinen *et al*., 2003; Kurnitski, 2001). Determining the air velocity within a crawl space is a complex issue, as higher air velocity can lead to increased evaporation of moisture from the bottom of the structure (Kurnitski, 2000).

Various dirt and contaminants, such as mold spores, can enter the crawl space through the supply air and settle on the surfaces of the foundation walls or ceiling structure. The probability of spore deposition may increase if the air in the crawl space remains for more extended periods. Spores require suitable conditions for their growth and development, with spore germination potentially occurring at relative humidity levels as low as 60%. However, active growth is only evident at a relative humidity of 75-85% (Balík, 2008). The study conducted by Viitenen et al. (2010) states that the critical ambient relative moisture for mold growth is 75% with a temperature range of 0-50 °C. The critical relative humidity levels are 90-95% for concrete and 75-80% for wood. Critical conditions can be understood as conditions with a risk of material degradation due to microbiological contamination. If mold growth and development occur in the crawl space, there is a risk of spore infiltration into the living space through leaks in the ceiling structure (Keskikuru *et al*., 2018; Airaksinen et al., 2004). If the crawl space is pressurized, the living space can draw air from the crawl space through leaks in the floor (crawl space ceiling structure). Molds can generally be divided into two categories: molds commonly found in the air and molds found on damp building materials. *Cladosporium* is common in the air, while *Penicillium* and *Aspergillus* are classified as soil fungi. *Aspergillus* versicolor is commonly found in damp buildings and can grow in materials with inferior nutrient content, such as concrete (Engelhart *et al*., 2002; Fog Nielsen, 2003; Jarvis and Miller, 2005). The occurrence of *Penicillium* in crawl spaces is reported, for example, in a study from Sweden by Bok *et al*. (2009).

In this study, the focus is on a comprehensive analysis of the microclimate of crawl space in the Czech Republic, where this type of foundation is not very common. In the Czech Republic, crawl spaces are gaining popularity in small timber structures. The conditions in which the wooden and wood-fiber elements of the ceiling structure of the crawl space were located were investigated. The microclimate behavior of crawl spaces in the Czech Republic is not well described; therefore, this research was carried out. The analysis of a family house involves continuous measurements (air temperature, relative humidity and air flow). The measured data were evaluated using statistical methods. The occurrence of mold can have a negative impact on the crawl space boundary structures, especially the wooden parts. Therefore, the crawl space of the house under study was swabbed for the presence of mold on the ceiling structure and foundation wall. Then, the crawl space was subjected to air age simulations, which can be used to estimate how long an imaginary particle remains within the crawl space. For example, an imaginary particle can be thought of as a mold spore that becomes trapped on the surfaces of a structure.

MATERIALS AND METHODS

The evaluation of the microclimate of the crawl space of a family house in the Czech Republic is divided into four basic parts. The first part is an experimental measurement of the crawl space. Subsequently, the measured data was subjected to statistical analysis to determine possible temperature and humidity differences between the tracts of the crawl space structure. The third part analyzes the potential presence of microorganisms, specifically molds, on the crawl space ceiling structure and foundation wall. The last part, air age, was simulated in the crawl space. It is the residence time of the imaginary particle in the crawl space that may indicate the possible capture of, for example, spores on the crawl space boundary structures. This study is a direct follow-up to the research conducted in the crawl space in October 2022, as described in Pobucká et al. (2024). Swabs of microorganisms on the structures were conducted, and temperature and humidity monitoring of the space was performed.

Measurements

The house is built on a crawl space foundation with two floors above ground. The floor plan of the house is rectangular with dimensions of 10.680 × 6.740 meters (Fig. 1). The foundation walls of the crawl space are constructed of concrete blocks. The height of the crawl space is 1,200 mm (from the bottom of the crawl space to the ceiling structure). The bottom of the crawl space is approximately 750 mm below the surrounding ground level. The bottom is covered with a geotextile on which the aggregate is placed. The ceiling is made of wooden beams with fiberboard sheathing. The *U-value* of the ceiling structure of the crawl space is 0.115 $W/(m^2K)$. A central foundation wall divides the crawl space lengthwise, creating two tracts of 23.6 m^2 (small tract) and 36.4 m^2 (large tract), respectively. There are vents in the surrounding foundation walls to allow natural ventilation of the crawl space. The area around the house is flat.

The microclimate in the crawl space was monitored using temperature and humidity sensors (Omega PLTH). The sensors were placed on the ceiling structure of the crawl space. Hot-wire thermoanemometers (Almemo FVAD 35) were placed in two selected vents to monitor the air flow. The vents marked in red in Fig. 1 are fully open and are not covered by any net or other cover. Data was recorded at 15-minute intervals. The location of the sensors is shown in Fig. 1.

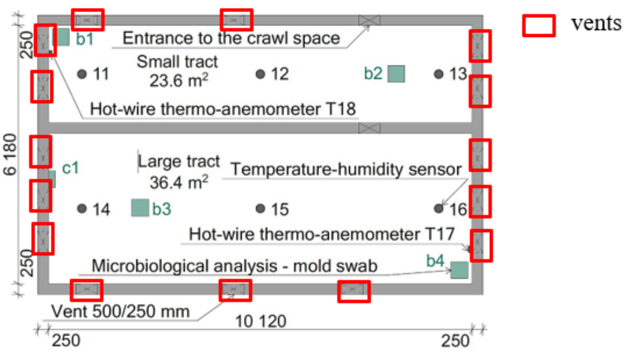

Fig. 1 The location of the sensors in the crawl space.

External climate conditions were measured using Mobile Alerts sensors located approximately 700 m from the monitored timber structure. The direction and speed of the external wind were measured at a height of 4.5 meters above the ground. Measurements were taken between April 2022 and August 2023. The average values from three sensors of the small tract and three sensors of the large tract were used in the calculations. The reason for this was to capture temperature and humidity within the entire tract.

Statistical analysis

The behavior of the small and large crawl space tracts was analyzed. Of particular interest is the conformity assessment between the series observed in small and large crawl space tracts, as well as the identification of any significant differences, especially concerning possible shifts in measured quantities. This concerns both the relative humidity and the air temperature.

Let us denote X_t^S and X_t^L as the time series of the quantity of interest, whether it be air temperature or relative humidity, observed at small and large tracts, respectively. We may assume the following decomposition (1).

$$X_t^S = m_t^S + E_t^S, X_t^L = m_t^L + E_t^L, \tag{1}$$

where m_t^S, m_t^L are deterministic functions of time, and E_t^S and E_t^L are zero-mean random processes. Hence, E_t^S and E_t^L represent random deviations from the means m_t^S and m_t^L at time t. If the two series X_t^S and X_t^L differ only by a shift in their means, we have $m_t^S = m_t^L + m$. Nevertheless, a more general form of m is possible. Particularly, the mean difference can be time-dependent, i.e., we have $m_t^S = m_t^L + m_t$. When dealing with meteorological data, this naturally arises as the means fluctuate with annual and/or other periods. Moreover, it is typical in the Czech Republic that there are greater differences between day and night temperatures in summer than in winter periods. Similarly, this also holds for relative humidity. Significantly different observations in the large tract would then result in values *of* m_t that significantly differ from zero. that are significantly different from zero. We are mainly interested in testing two substantially related hypotheses:

1. It is expected that the mean relative humidity in the small tract should be higher than in the large tract.
2. Similarly, we may expect that the size of the space could have a negative effect on the air temperature.

The inference about m_t can be made based on the series of differences $Y_t = X_t^S - X_t^L = m_t + E_t$, where E_t is again zero-mean random noise. In the first approach, we summarize the basic characteristics of a particular series, i.e., their means, standard deviations, or maxima, observed during different year seasons. In the following, we apply techniques of time series analysis for the estimation of m_t. Specifically, we consider a regression model with seasonal components of the form (2).

$$m_t = \beta_0 + \sum_{i=1}^{k} \left(a_i \cos\frac{2\pi t}{T_i} + b_i \sin\frac{2\pi t}{T_i} \right) \tag{2}$$

with regression parameters β_0, a_i, b_i for $i=1, \ldots, k$, where k is the number of periods T_i incorporated into the model. The periods can be identified using a periodogram in combination with Fisher's test to determine their significance, see e.g. Shumway & Stoffer (2017). The estimates of parameters in the model are commonly obtained using the Ordinary Least Squares (OLS) method. Based on the covariance matrix of the estimated parameters, we can evaluate confidence intervals for m_t at a given time t and decide hereby about the significance of the difference m_t^S - m_t^L. However, the covariance structure of the noise E_t, particularly its serial correlation, may negatively influence the quality of the estimates. This comprises both the parameters and their variability. Here, we consider the ARMA (*p, q*) model for the random process E_t, and apply the Cochrane-Orcutt procedure to adjust the OLS estimates above, for details see Brockwell and Davis (2016).

Microbial analysis of the ceiling structure and foundation wall

The presence of microorganisms on the ceiling structure and foundation wall was analyzed. The swab was taken in May 2023 using a 100 cm^2 stencil with a wipe sponge – BIOING, SR18-10BPW-G. No sterilization methods have been carried out in the crawl space since sampling in October 2022. Nevertheless, the air age is indicative not only of assessing growth conditions for any molds already present before April 2022 but also in terms of quantifying the likelihood that any incoming organism is captured in space. The test sponge was moistened with peptone water to improve adhesion to the surface. The sampling was conducted in accordance with EN ISO 18593 (2019). The sponge was aseptically removed from its protective packaging and pressed against the wall with moderate pressure. It was then moved, both vertically and horizontally, to collect the sample. The sponge was then resealed in its protective packaging without exposure to air to prevent contamination of the sample. The sample was transported to the laboratory within 24 hours in a cool box maintained at 1-8°C (Pobucká *et al.*, 2024). Fig. 2 shows the sampling process.

a) b)

Fig. 2 Sampling template on the a) ceiling structure and b) foundation wall.

Process of cultivation of isolates:

- In the laboratory, the sample was placed in 40 ml of sterile saline solution and shaken in a Stomacher homogenizer for 1 minute.
- One milliliter of the solution was inoculated onto Petri dishes (dish diameter 90 mm) with Chloramphenicol Glucose Agar for the selective detection of yeasts and molds. Furthermore, 0.1 ml of the solution was inoculated onto a Petri dish with PCA (Plate Count Agar) for the enumeration of live, culturable heterotrophic microorganisms, including bacteria, yeasts, and molds. Petri dishes were inoculated in two replicates.
- Plate Count Agar was incubated for 72 hours at 30°C.
- Chloramphenicol-glucose agar was incubated for 5 days at 25 °C.
- The number of microorganisms was expressed as colony-forming units per 100 cm^2 - CFU/100 cm^2.
- The sample was further subjected to identification; therefore, morphologically distinguishable colonies of filamentous fungi were subcultured. Subculturing was performed with Chloramphenicol Glucose Agar at 25 °C.
- To investigate the microscopic morphology of the fungi, a seven-day culture grown on Malt Extract Agar (MEA, Oxoid^{TM}) in the dark at 25 °C was established. Macroscopic morphological characters were examined on seven-day-old cultures grown on Sabouraud dextrose agar (Oxoid^{TM}) at 25 °C in the dark (Pobucká *et al.*, 2024).

Numerical simulation in crawl space

The age of the air in the crawl space was simulated for westerly and easterly air flows. The westerly direction was chosen because it corresponds to the prevailing wind direction at the site. The eastern direction was chosen because of the fence near the house, which can affect the air flow within the crawl space. The fence consists of a gabion wall with a wooden infill that restricts air flow. The speed, 1.0 m/s, was set at a height of 4.5 m above the ground to compare the air distribution in the two cases. The RANS (Reynolds-averaged Navier-Stokes) turbulent model was employed in the simulations, along with the *k*- *ε* model. Reynolds decomposition is used to derive the RANS equations (Zhang *et al.*, 2020) of the form of the resulting equations (3), (4), (5).

$$\frac{\partial \bar{u}_i}{\partial x_i} = 0 \tag{3}$$

$$\frac{\partial \bar{u}_i}{\partial t} + \frac{\partial}{\partial x_j}\left(\bar{u}_i \bar{u}_j\right) = -\frac{1}{\rho}\frac{\partial \bar{p}}{\partial x_i} + \frac{\partial}{\partial x_j}\left(2v\bar{s}_{ij}\right) - \frac{\partial}{\partial x_j}\left(\overline{u_i' u_j'}\right) \tag{4}$$

$$\frac{\partial \bar{c}}{\partial t} + \frac{\partial}{\partial x_j}\left(\bar{c}\bar{u}_j\right) = \frac{\partial}{\partial x_j}\left(D\frac{\partial \bar{c}}{\partial x_j}\right) - \frac{\partial}{\partial x_j}\left(\overline{c' u_j'}\right) \tag{5}$$

Where: *t* denotes time, *p* is the instantaneous pressure, *v* is the kinematic molecular viscosity, $\bar{s}_{ij}$ is the strain-rate tensor, *c* the instantaneous concentration, *D* the molecular diffusion coefficient and x_i, u_i the instantaneous position and velocity. Next, $(\overline{c' u_j'})$ is the turbulent mass flux and $(\overline{u_i' u_j'})$is the Reynolds stress. The logarithmic wind law was used for the outdoor air flow, i.e., wind speed increases logarithmically with height. The difference in air pressure indicates wind speed; the greater the gradient, the faster the air flow is (Mareike *et al.*, 2014; Solari, 2019; Zhang *et al.*, 2020).

$$u(z) = \frac{u_*}{\kappa}\ln\left(\frac{z}{z_0}\right), \tag{6}$$

Where: u is the longitudinal wind speed, u_* is the frictional velocity, z_0 is the roughness height and κ is the von Kármán constant. The terrain around the object was included in the simulation using the terrain parameter z_0 (0.05 m). A simplified house model was created for the simulation and a steady-state isothermal model was established. The convergence margin was set at 10^{-3}. The domain size was chosen to be *5H* upstream, *15H* downstream and *5H* lateral distance. The value of *H* is the height of the building. The simulations were performed by OpenFOAM software. The model was validated against the measured data. (Tominaga *et al.*, 2008; Abu-zidan *et al.*, 2021; Pobucká *et al.*, 2024). Subsequently, the age of the air in the crawl space was calculated as a post process of the air flow. The transport equation (7) is used to calculate the age of the air in space, (Hayashi *et al.*, 2002; Li *et al.*, 2003).

$$\frac{\partial}{\partial x}(u\tau) + \frac{\partial}{\partial y}(v\tau) + \frac{\partial}{\partial z}(w\tau) = \frac{\partial}{\partial x}\left(D\frac{\partial \tau}{\partial x}\right) + \frac{\partial}{\partial y}\left(D\frac{\partial \tau}{\partial y}\right) + \frac{\partial}{\partial z}\left(D\frac{\partial \tau}{\partial z}\right) + 1, \tag{7}$$

Where: *D* is the diffusion coefficient in m^2/s, *u* is average speed in the *x* direction in m/s, *v* is average speed in the *y* direction in m/s, *w* is the average speed in the *z* direction in m/s and *τ* is age of air in seconds.

RESULTS AND DISCUSSION

Air flow

Hot-wire thermoanemometer T17 was in the vent on the east side (large tract) and hot-wire thermoanemometer T18 was in the vent on the west side (small tract). The average air flow was 0.45 m/s (sensor T17) and 0.36 m/s (sensor T18). Whereas the outdoor air flow reached up to 2.2 m/s, the air flow in the vents ranged from 0.10 to 0.75 m/s.

Air temperature

In the next step, we analyze the data from the temperature-humidity sensors placed in the crawl space. From the 15-minute records we determine the corresponding daily averages. Trajectories of daily air temperatures observed in the small and large tracts are shown in Fig. 33. The path of differences (Fig. 3) suggests overall higher temperature in the large tract. Nevertheless, the magnitude of the difference varies between year seasons, being less significant during the winter period. A summary of the fundamental characteristics of each season is provided in Table 1. There is considerable variation in the mean between winter and summer, most notable for summer 2023. Even more important are the deviations on the daily scale, as expressed by the maximum in Table 1. On a particular day in autumn 2022, the difference reached up to 0.31 °C. Notice that the standard deviations in Tab. 1 are evaluated under the assumption of constant mean in the given period, i.e., in case of significant non-stationarity of the series, are the values markable overestimated.

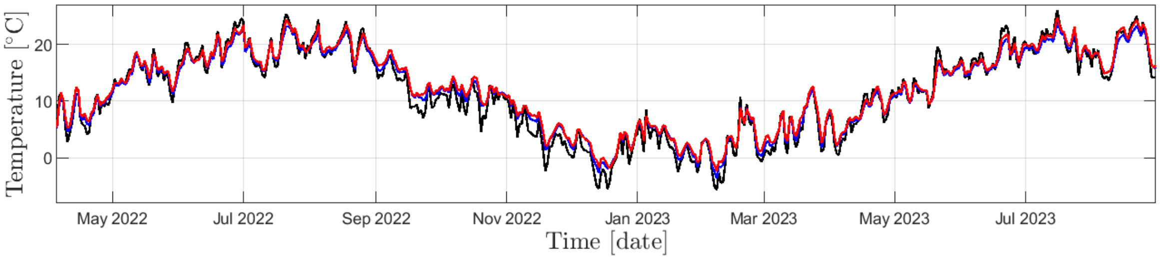

Fig. 3 Daily air temperatures in the small (blue) and large (red) crawl space, outdoor air temperature (black).

Tab. 1 Overview of basic characteristics for each period.

Temperature differences [°C]	Spring from 5.4.2022	Summer 2022	Autumn 2022	Winter 2022	Spring 2023	Summer to 31.8.2023
Mean	-0.48	-0.50	-0.39	-0.34	-0.38	-0.57
Standard deviation	0.31	0.30	0.36	0.38	0.20	0.40
Maximum	0.03	0.13	0.31	0.29	0.06	0.14

Inference on daily differences is conducted based on a seasonal regression model with ARMA errors from Sect. Statistical analysis of the data. We consider only the presence of annual periodicity, yielding the mean of the form $\boldsymbol{m_t = \beta_0 + a_1 \cos\frac{2\pi t}{365} + b_1 \sin\frac{2\pi t}{365}}$. Other harmonic components identified using a periodogram have, however, not clear meaning and their interpretation within the context of a crawl space is problematic. Namely, these correspond to periods 36, 13, 15, and 20 days. Such periodicities arise most likely because of our simplified assumption on stationarity of the random noise.

Nevertheless, our computations have shown that the conclusions regarding the significance of the temperature difference remain the same even when such periodicities are incorporated into the model. As discussed in Sect. Statistical analysis of the data reveals that the OLS estimates are biased due to the presence of serial correlation in the errors and require adjustment using the Cochrane-Orcutt procedure. For this purpose, we consider ARMA (1,0) process for the random errors, i.e., we suppose $\boldsymbol{E_t = \varphi_1 E_{t-1} + W_t}$ with white noise W_t.

The parameter estimates (std. error) for the simplest annual model are: $\beta_0 = -0.438$ (0.0012), $a_1 = 0.047$ (0.0022), $b_1 = -0.098$ (0.0024), $\varphi 1 = 0.678$ (0.0287). Based on the estimated covariance matrix, we evaluate for all time points t the 95% confidence interval for m_t. This is illustrated in Fig. 4. The lower plot in Fig. 4 displays the variant with all incorporated harmonic components. In neither case does the confidence interval cover the zero value; hence, the difference between mean temperatures in small and large tracts is significant.

The mean average air temperature was 11.97 °C (small tract) and 12.41 °C (large tract). The air temperature in the crawl space was up to 3°C lower in summer 2022 and 3.8°C lower in summer 2023 than the outdoor air temperature.

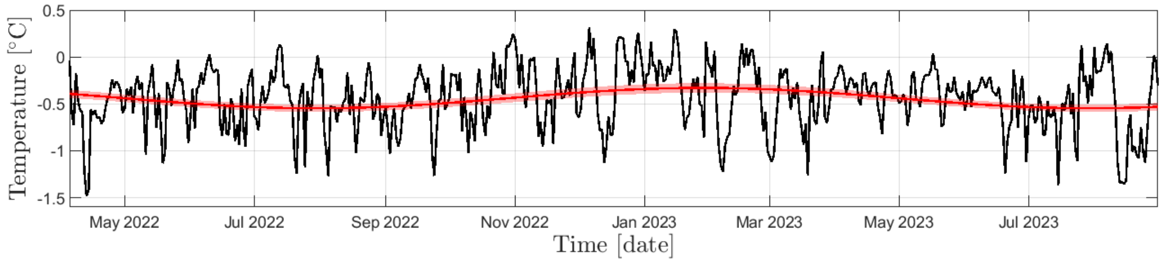

Fig. 4 Differences in daily air temperature values in the small and large wings of the crawl space.

Relative humidity

The same analysis was performed in the context of observed relative humidity. Trajectories of daily averages are shown in Fig. 5. The paths of the different series (Fig. 6) suggest that the relative humidity is overall higher in small tracts, with season-dependent deviations. However, the plot also shows some interannual progress (compare the left and right parts of Fig. 5).

Basic descriptive characteristics for particular seasons are given in Tab. 2. While relative humidity in particular tracts changes during the year, the differences between small and large tracts are quite similar in summer or winter. Nevertheless, the year-to-year fluctuations are remarkable, mostly evident for the two summer seasons. Notable are also the daily differences between tracts; its daily maximum was almost 10% in the summer of 2023 and remained relatively stable at around 8% in 2022.

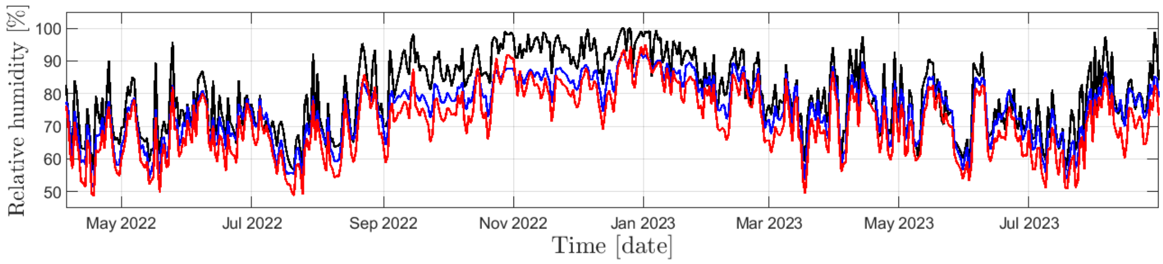

Fig. 5 Daily air relative humidity in the small (blue) and large (red) crawl space, outdoor air temperature (black).

Tab. 2 Overview of basic characteristics for each period.

Rel. humidity differences [%]	**Spring from 5.4.2022**	**Summer 2022**	**Autumn 2022**	**Winter 2022**	**Spring 2023**	**Summer to 31.8.2023**
Mean	3.33	3.85	3.44	3.33	4.37	5.49
Standard deviation	1.60	2.14	2.63	2.27	1.26	1.85
Maximum	7.09	8.11	8.12	7.50	8.95	9.82

For statistical inference on the mean difference mt we consider again the regression model with ARMA (1.0) errors. We base it on model (2). However, the presence of a non-seasonal systematic component requires its modification. Specifically, we can consider a trend in the form of a polynomial. Considering the annual periodic component and linear trend, we obtain the model $\boldsymbol{m_t = \beta_0 + \beta_1 t + a_1 \cos\frac{2\pi t}{365} + b_1 \sin\frac{2\pi t}{365}}$. The estimated mean function is shown in Fig. 6, together with a 95% confidence bound evaluated at a particular time point. The parameter estimates (std. error) for the simplest annual model are: $\beta_0 = 2.818$ *(0.1699)*, $\beta_1 = 2.818$ *(0.1699)*, $a_1 = 0.101$ *(0.0880)*, $b_1 = 0.699$ *(0.0864)*, $\varphi 1 = 0.686$ *(0.0265)*. Here follows the conclusion that the relative humidity in the small tract is significantly higher over the whole monitored period.

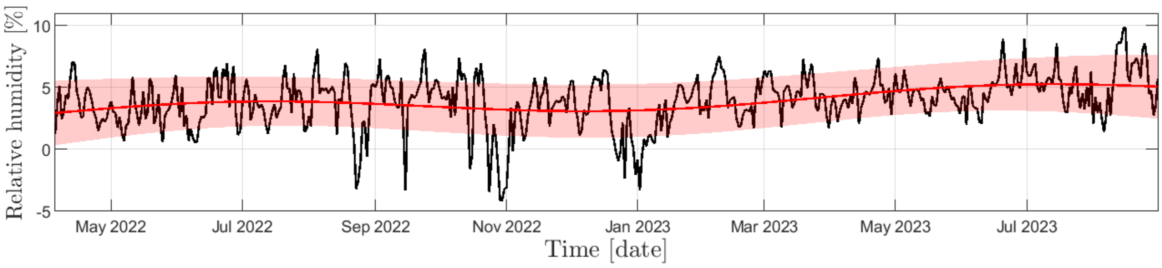

Fig. 6 Differences in daily relative humidity values in the small and large wings of the crawl space.

The mean average relative humidity was 75.50% (small tract) and 71.60 % (large tract). The highest relative humidity values were measured during December, reaching 90.20% in the crawl space. During the summer, the average relative humidity in the crawl space ranged from 55 to 85%.

High humidity poses one of the possible risks to the structural parts of the crawl space, particularly the ceiling structure. The temperature in the crawl space during the summer months can be lower than the outside temperature. This temperature difference is due to the thermal capacity of the crawl space structure, which delays the equalization of air temperature between the outside environment and the crawl space. Consequently, this can lead to unstable and risky humidity conditions within the crawl space (Matilainen and Kurnitski, 2003; Sato and Nakajima, 2018; Airaksinen *et al*., 2020). Studies performed by Matilainen and Kurnitski (2003) and Vanhoutteghem *et al*. (2017) examine the impact of the thermal capacity of the ceiling structure on the microclimate in the crawl space. When reducing the *U-value* by half (from 0.4 to 0.2 W/(m^{2}K)), the relative humidity in the crawl space was 10% higher and the air temperature was on average 2°C lower.

The conclusions drawn from this study from the Czech Republic are consistent with the results of some other foreign studies. For example, it confirms that the air temperature within the crawl space tends to be lower than the outdoor air temperature during the summer months, while the relative humidity within the crawl space remains high, typically around 80%.

Microbial analysis

Microbiological analysis of the ceiling and wall structure was carried out in May 2023. Four samples were taken on the fiberboard ceiling structure. The location of the swabs is shown in Fig. 1. For this analysis, the west wall of the crawl space was selected, where moisture was frequently observed on the surfaces. The results are presented in Tab. 3. The results were read from the colonies shown in Fig. 7.

Tab. 3 Numbers of colony forming units (CFU/100 cm^2) of molds isolated, cultivated on PCA.

Marking of sampling point	CFU/100 cm^2		
	Yeast	Molds	Total
c1	3,253	973	1,018
b1	40	1,347	1,387
b2	200	1,000	1200
b3	13	213	226
b4	987	27	1,014

A significant number of yeasts were observed on the foundation wall compared to the ceiling structure. Conversely, the highest number of molds was recorded on the ceiling structure for samples b1 and b2 (small tract of the crawl space). The high number of microorganisms at the foundation wall is attributed to the porosity of the concrete, as observed in sample c1. Fig. **7** shows isolates of microscopic fungi (molds). The isolates were cultured on a Chloramphenicol Glucose Agar medium. Inoculation of Petri dishes was done in two replicates. From the isolates in Fig. 7, it can be seen that the frequency of fungal colonies is not high, and the values in Tab. 3. correspond to this. It must also be said that the molds were present on the foundation wall in the form of spores. No visible mold growth was observed. The colonies found in Fig. 7 and

Fig. **8** were cultured under ideal laboratory conditions.

c1 b1 b2 b3 b4

Fig. 7 Isolation of fungal community from the ceiling structure and wall, medium Chloramphenicol Glucose Agar.

To determine the fungal genera, the isolates from Fig. 7 were cultured separately as seven-day-old cultures. The isolates of microscopic fungi were subjected to identification and assigned to the genus. *Penicillium*, *Aspergillus* and *Cladosporium* were most abundant in the samples on both the ceiling structure and the foundation wall. Furthermore, the genera were identified *Ramularia* or *Stereum*. Tab. 4 shows the specific genera of fungi at the sampled locations in the structure.

Tab. 4 Identification of molds at sampling points in the structure.

Marking of sampling point	Identification of molds
c1	*Penicillium sp., Cladosporium sp., Aspergillus sp.*
b1	*Penicillium sp., Cladosporium sp.*
b2	*Fusarium sp., Stereum sp.*
b3	*Cladosporium sp., Ramularia sp.*
b4	*Penicillium sp.*

Fig. **8** shows photographs of the isolates from the front of the Petri dish, as well as their microscopic morphology. The occurrence of mold in crawl spaces has been the subject of numerous studies. The *Penicillium* is the dominant genus within crawl spaces. Furthermore, the genus *Cladosporium* and *Aspergillus* were identified. The dominance of the *Penicillium* genus is attributed to the smaller size of its spores facilitating better dispersion in the air compared to *Cladosporium* spores, for example (Airaksinen *et al*., 2004; Bok *et al*., 2009).

Penicillium can grow on different types of material – concrete, wood, wooden panels, drywall or ceramics (Hyvärinen *et al*., 2002). Especially on dry summer days, airborne spores of *Cladosporium* appear in the air (Malíř and Ostrý, 2003).

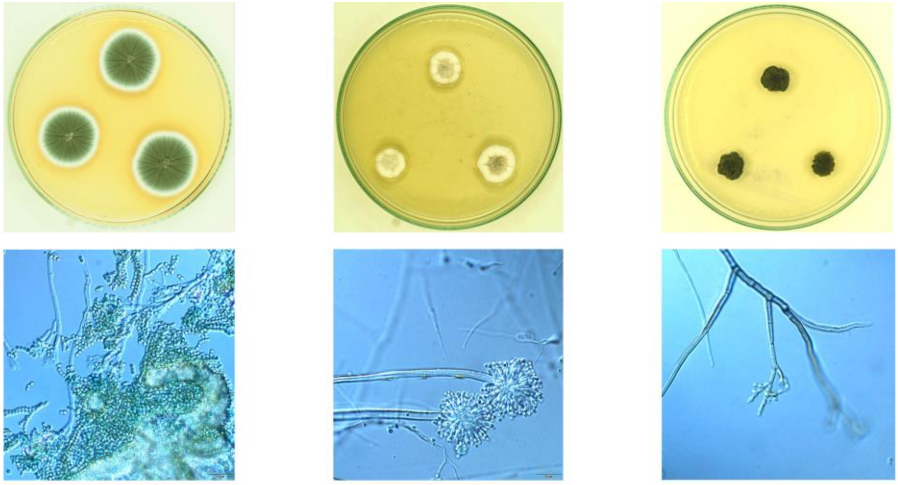

a) Penicillium sp. b) Aspergillus sp. c) Cladosporium sp.

Fig. 8 Identification of selected isolates, microscopic morphology, seven-day-old cultures.

Air age simulation

Air age simulations were performed to determine how long the air can linger in the crawl space. The outside air in the crawl space also introduces debris that can adhere to the surfaces of the structure. The longer the air stays in the crawl space the greater the potential for debris to be trapped on the structure. The air age was simulated in the monitored crawl space. Fig. 5 shows the simulation at an air speed (velocity) of 1.0 m/s from the west and from the east, respectively, performed at the level of the ceiling structure. Due to the asymmetric arrangement of the vents, the air flow from the west and east differs. In the smaller tract, the air remained longer, both when coming from the west and when coming from the east. The maximum air age value for the air flow from the west was 477 s (7.95 minutes) and from the east 346 s (5.77 minutes). The average values are summarized in Tab. 5.

Tab. 5 Average age of air in the entire crawl space in minutes.

Crawl space	Age of air in westerly flow in minutes (seconds)	Age of air in easterly flow in minutes (seconds)
Small tract	4.4 (265.8)	4.2 (249.6)
Large tract	2.6 (156.5)	2.6 (153.6)

The simulation in Fig. 9 is performed at the level of the ceiling structure. It identified potential risk points in the structure, particularly at the corners. Interestingly, a larger quantity of microorganisms was found in the small tract, where a greater age of air was also observed compared to the large tract, Tab 5.

The red spots in the simulations indicate where the air remained longest within the structure. These were mainly the corners of the structure, and these locations also contained high numbers of microorganisms, as seen in samples b1 and b4. The specific microorganism counts were 1,387 (b1) and 1,014 (b4). High counts of microorganisms were also recorded for sample b2 (1,200). This site was red in the simulations during the westerly flow. A large number of microorganisms in sample b2 may be due to the prevailing westerly flow in the real structure, where the second part of the crawl space was less ventilated.

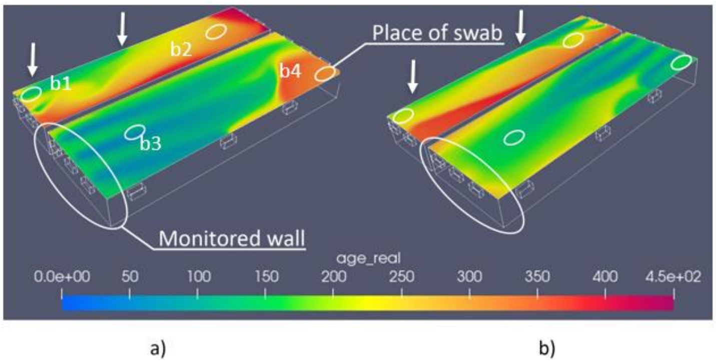

Fig. 9 Simulation of air age in the crawl space at an air velocity of 1.0 m/s, a) air flow direction from the west, b) air flow direction from the east. (Arrows indicate the vents).

Simulations of the age of the air on the foundation wall are shown in Fig. 10. The average air age values for the foundation wall are shown in Tab. 6. The highest average values were found for the wall when the air flow was from the east in the large tract, namely 285.1 seconds (4.8 minutes). The location of the vents is not symmetrical in the small and large tracts. This may have caused differences in airflow in individual tracts. In the large tract, due to the location of more vents, air was able to enter the space more easily, and thus better ventilation was possible. In the small wing, the vents were located near the inner corner of the structure, causing air to be drawn out of the structure through the nearest vent and making it difficult for air to enter the crawl space.

Tab. 6 Average age of air at foundation wall crawl space in minutes.

Crawl space	Age of air in westerly flow in minutes (seconds)	Age of air in easterly flow in minutes (seconds)
Small tract	4.3 (254.5)	4.2 (249.5)
Large tract	2.2 (129.8)	4.8 (285.1)

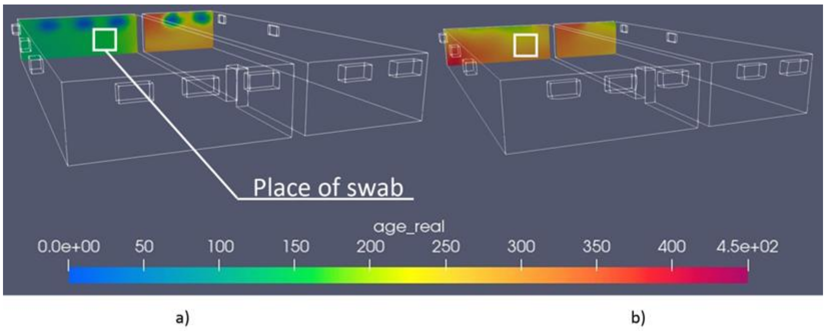

Fig. 10 Simulation of air flow in the crawl space at an air velocity of 1.0 m/s, cross section at the location of the swab (view of the monitored wall), a) air flow direction from the west, b) air flow direction from the east.

The age of the air reflects the air flow pattern in space (Li *et al.*, 2003). Air age is defined as the time elapsed since the air entered space (Sandberg, 1981; Sandberg and Sjöberg, 1983). There are three methods to measure the age of air: the decay method, the source method, and the pulse method. Tracer gas methods are reliable but time-consuming. These methods are not suitable for ventilation systems with multiple rooms and multiple ducts. Larger ventilation systems must be solved numerically using the

Computational Fluid Dynamics (CFD) method. Air age simulation proved to be a valuable tool for an initial assessment of the crawl space, identifying potential problem areas within the structure.

Airflow, air temperature, and relative humidity were monitored in the study. In addition, a microbic analysis of the structure was performed, and the study concluded with simulations of air shedding. The air age simulation model was validated using airflow measurements. Relative humidity and air temperature measurements in the crawl space tract highlighted the possible different temperature and humidity behavior of the crawl space. The results of the mathematical analysis indicated higher relative humidity and lower air temperature in the small tract. These conditions may lead to higher water vapor condensation in the small tract, creating favorable conditions for mold growth. Higher numbers of microorganisms (samples b1 and b2) were found in the small tract than in the large tract. The air age simulation revealed higher air stagnation in the small tract compared to the large tract under both westerly and easterly airflow conditions.

Furthermore, the simulations indicated that the corners of the structure, where air could stay, could stay longer than in the crawl space. This was supported by the results of the microbial analysis, which showed that the numbers of microorganisms found in the corners were 1,387 (b1) and 1,014 (b4).

It is evident from the analysis that the crawl space partitioning (central foundation wall) can cause different microclimatic environments in the crawl space. Specifically, the various temperature and humidity behaviors of the crawl space tracts under study. This can be mitigated by designing, for example, center foundation piers that connect the entire crawl space. Furthermore, from the air age simulations, it was possible to observe air being exhausted through vents located near the corners. It was difficult for air to enter the crawl space. Therefore, it is not advisable to place the vents close to the corners of the structure. The standard (International Residential Code, 2018) specifies that the ventilation opening must be located a minimum of 915 mm from the inner edge of the structure. Before designing a crawl space, it is undoubtedly advisable to know the location, such as the prevailing wind direction, the location of the fence, or the garden concept (e.g., tall shrubs, a garden house). These can all influence the airflow in the structure. It is undoubtedly advisable for the owner to check the space regularly for mold growth or to ensure the vents are fully uncovered (for example, by not placing pots in front of them).

CONCLUSION

This paper examines the analysis of the crawl space microclimate in a timber building located in the Czech Republic. The relative humidity in the cellars reached up to 85% in the summer and 90% in the winter, humidity that can lead to mold growth. High humidity can lead to structural degradation, particularly of the wooden components in the crawl space. The behavior of the microclimate in the crawl space can be influenced by the central foundation wall, which divides the crawl space into two sections. The measurements also revealed significant differences in relative humidity between the crawl space tracts, with the smaller tract exhibiting higher humidity levels than the larger tract. The small tract was found to have higher air age values, a higher number of microorganisms, and a higher relative humidity. The results suggest that the distribution of the structure may have a significant effect on crawl space behavior.

The air age simulation identified potential risk locations in the crawl space where the air remained the longest. These were mainly the corners of the structure and the space along the center wall (in the small tract). This method also showed how long the air could stay near the crawl space and highlighted the potential risk of trapping mold spores. An experimental analysis revealed the presence of *Penicillium*, *Aspergillus*, and *Cladosporium* mold spores in the crawl space. There was no visible mold growth on the structures. It is particularly important to control the wooden elements in this environment, which can be degraded by prolonged exposure to high humidity.

The crawl space system is not standard in Central Europe, yet we do encounter this type of building foundation in the Czech Republic, for example. It is essential to observe the behavior of the crawl space microclimate and identify potential risks associated with construction in these conditions so that they can be mitigated during the design phase. This approach has been guided by recommendations from abroad to date.

REFERENCES

Abu-zidan, Y., Mendis, P., Gunawardena, T., 2021. Optimising the computational domain size in CFD simulations of tall buildings. Heliyon, 7(4), e06723-e06723. https://doi.org/10.1016/j.heliyon.2021.e06723

Airaksinen, M., Kurnitski, J., Pasanen, P., Seppänen, O., 2004. Fungal spore transport through a building structure. Indoor air, 14(2), 92-104. https://doi.org/10.1046/j.1600-0668.2003.00215.x

Airaksinen, M., Olsson, L., Kurnitski, J., Hvidberg, S., 2020. Highly insulated crawl spaces with controlled minimal ventilation - Proof of concept by field measurements. E3S Web of Conferences, 172, 7004. https://doi.org/10.1051/e3sconf/202017207004

Airaksinen, M., Kurnitski, J., Seppanen, O., Airaksinen, M., 2003. On the crawl space moisture control in buildings. Proceedings of the Estonian Academy of Sciences: Engineering, 9(1), 34-58. http://search.proquest.com/docview/27909883/

Annila, P., Lahdensivu, J., Suonketo, J., Pentti, M., Vinha, J., 2018. Need to repair moisture- and mold damage in different structures in finnish public buildings. Journal of Building Engineering, 16, 72. https://doi.org/10.1016/j.jobe.2017.12.010

Balík, M., 2008. Odvlhčování staveb (2., přeprac. vyd), [Dehumidification of buildings (2nd, revised ed.)]. Grada.

Bok, G., Hallenberg, N., Åberg, O., 2009. Mass occurrence of Penicillium corylophilum in crawl spaces, south Sweden. Building and environment, 44(12), 2413-2417. https://doi.org/10.1016/j.buildenv.2009.04.001

Brockwell, P., Davis, R., 2016. Introduction to time series and forecasting (Third edition). Springer.

Burke, S., 2007. Crawl spaces in wood framed single family dwellings in Sweden: unwanted yet popular, 10. https://doi.org/10.1108/02630800710740976

ČSN EN ISO 18593. 2019. Mikrobiologie potravinového řetězce - Horizontální metody specifikující techniky vzorkování z povrchů. Úřad pro technickou normalizaci, metrologii a státní zkušebnictví [Microbiology of the food chain - Horizontal methods specifying surface sampling techniques. Office for Technical Standardization, Metrology and State Testing].

Engelhart, S., Loock, A., Skutlarek, D., Sagunski, H., Lommel, A., Färber, H., Exner, M., 2002. Occurrence of Toxigenic Aspergillus versicolor Isolates and Sterigmatocystin in Carpet Dust from Damp Indoor Environments. Applied and Environmental Microbiology, 68(8), 3886-3890. https://doi.org/10.1128/AEM.68.8.3886-3890.2002

Erickson, B., Zhai, Z., 2008. Evaluation of ventilation code requirements for building crawl spaces. Building simulation, 1(4), 311-325. https://doi.org/10.1007/s12273-008-8325-3

Fog Nielsen, K., 2003. Mycotoxin production by indoor molds. Fungal Genetics and Biology, 39(2), 103-117. https://doi.org/10.1016/S1087-1845(03)00026-4

Hayashi, T., Ishizu, Y., Kato, S., Murakami, S., 2002. CFD analysis on characteristics of contaminated indoor air ventilation and its application in the evaluation of the effects of contaminant inhalation by a human occupant. Building and environment, 37(3), 219-230. https://doi.org/10.1016/S0360-1323(01)00029-4

Hyvärinen, A., Meklin, T., Vepsäläinen, A., Nevalainen, A., 2002. Fungi and actinobacteria in moisture-damaged building materials-concentrations and diversity. International biodeterioration, biodegradation 49(1), 27-37. https://doi.org/10.1016/S0964-8305(01)00103-2

International Residential Code, 2018. USA, https://codes.iccsafe.org/content/IRC2018P6

Jarvis, B., Miller, J., 2005. Mycotoxins as harmful indoor air contaminants. Applied microbiology and biotechnology, 66(4), 367-372. https://doi.org/10.1007/s00253-004-1753-9

Keskikuru, T., Salo, J., Huttunen, P., Kokotti, H., Hyttinen, M., Halonen, R., Vinha, J., 2018. Radon, fungal spores and MVOCs reduction in crawl space house: A case study and crawl space development by hygrothermal modelling. Building and environment, 138, 1-10. https://doi.org/10.1016/j.buildenv.2018.04.026

Kurnitski, J., 2000. Crawl space air change, heat and moisture behaviour. Energy and buildings, 32(1), 19-39. https://doi.org/10.1016/S0378-7788(99)00021-3

Kurnitski, J., 2001. Ground moisture evaporation in crawl spaces. Building and environment, 36(3), 359-373. https://doi.org/10.1016/S0360-1323(00)00013-5

Kurnitski, J., Matilainen, M., 2000. Moisture conditions of outdoor air-ventilated crawl spaces in apartment buildings in a cold climate. Energy and buildings, 33(1), 15-29. https://doi.org/10.1016/S0378-7788(00)00061-X

Laukkarinen, A., Vinha, J., 2017. Temperature and relative humidity measurements and data analysis of five crawl spaces. Energy Procedia, 132, 711-716. https://doi.org/10.1016/j.egypro.2017.10.011

Li, X., Li, D., Yang, X., Yang, J., 2003. Total air age: an extension of the air age concept. Building and environment, 38(11), 1263-1269. https://doi.org/10.1016/S0360-1323(03)00133-1

Lynn, M., Overstreet, G., Brack, H., Wayne R., T., 2011. Crawl spaces as reservoirs for transmission of mold to the livable part of the home environment. Reviews on environmental health, (263, p.205-213. https://doi.org/10.1515/reveh.2011.028

Malíř, F., Ostrý, V., 2003. Vláknité mikromycety (plísně), mykotoxiny a zdraví člověka (Vyd. 1). Národní centrum ošetřovatelství a nelékařských zdravotnických oborů [Filamentous Micromycetes (Molds), Mycotoxins and Human Health (Ed. 1). National Center for Nursing and Non-Medical Health Professions].

Mareike, K., Ralf, P., Sven, P., Joachim, S., 2014. City and wind: climate as an architectural instrument. Berlin: DOM Publishers.

Matilainen, M., Kurnitski, J., 2003. Moisture conditions in highly insulated outdoor ventilated crawl spaces in cold climates. Energy and buildings, 35(2), 175-187. https://doi.org/10.1016/S0378-7788(02)00029-4

Pobucká, S., Kalhotka, L., Laichmanová, M., Šuhajda, K., 2024. Monitoring of Microclimatic Conditions and The Occurrence of Micromycetes in Crawl Space. Acta Facultatis Xylologiae Zvolen, (661), 15. https://doi.org/10.17423/afx.2024.66.1.05

Pobucká, S., Kučírek, P., Šuhajda, K., Vorlíčková, P., Žajdlík, T., 2024. Numerical analysis of crawl spaces airflow. Juniorstav: Proceedings 26th International Scientific Conference Of Civil Engineering (pp. 1-8). Vysoké učení technické v Brně, Fakulta stavební. https://doi.org/10.13164/juniorstav.2024.24073

Risberg, M., Westerlund, L., 2020. Experimental investigation of a crawl space located in a sub-arctic climate. Results in Engineering, 7, 100158. https://doi.org/10.1016/j.rineng.2020.100158

Sandberg, M., 1981. What is ventilation efficiency?. Building and environment, 16(2), 123-135. https://doi.org/10.1016/0360-1323(81)90028-7

Sandberg, M., Sjöberg, M., 1983. The use of moments for assessing air quality in ventilated rooms. Building and environment, 18(4), 181-197. https://doi.org/10.1016/0360-1323(83)90026-4

Sato, Y., Nakajima,, Y., 2018. Study on humidity control method of high humidity environment in the crawl space in floor insulated house. ournal of Environmental Engineering (Transactions of AIJ), (83), pp. 901–11. https://doi.org/10.3130/aije.83.901

Shumway, R., Stoffer, D., 2017. Time series analysis and its applications: with R examples (Fourth edition). Springer International Publishing AG.

Solari, G., 2019. Wind Science and Engineering: Origins, Developments, Fundamentals and Advancements (1st ed. 2019). Springer International Publishing AG. https://doi.org/10.1007/978-3-030-18815-3

Tominaga, Y., Mochida, A., Yoshie, R., Kataoka, H., Nozu, T., Yoshikawa, M., Shirasawa, T., 2008. AIJ guidelines for practical applications of CFD to pedestrian wind environment around buildings. Journal of wind engineering and industrial aerodynamics, 96(10), 1749-1761. https://doi.org/10.1016/j.jweia.2008.02.058

Vanhoutteghem, L., Morelli, M., Sørensen, L., 2017. Can crawl space temperature and moisture conditions be calculated with a whole-building hygrothermal simulation tool?. Energy Procedia, 132, 688-693. https://doi.org/10.1016/j.egypro.2017.10.007

Viitanen, H., Vinha, J., Salminen, K., Ojanen, T., Peuhkuri, R., Paajanen, L., Lähdesmäki, K., 2010. Moisture and Bio-deterioration Risk of Building Materials and Structures. Journal of building physics, 33(3), 201-224. https://doi.org/10.1177/1744259109343511

Yuan, L., Takada, S., Fukui, K., 2024. Study on mold and condensation risks after vacancy of residential space with walls in contact with the ground. Journal of Building Engineering, 89, 109300. https://doi.org/10.1016/j.jobe.2024.109300

Zhang, X., Weerasuriya, A., Tse, K., 2020. CFD simulation of natural ventilation of a generic building in various incident wind directions: Comparison of turbulence modelling, evaluation methods, and ventilation mechanisms. Energy and buildings, 229, 110516. https://doi.org/10.1016/j.enbuild.2020.110516

ACKNOWLEDGMENT

Acknowledgments should be simply phrased and should include only brief references to research project or funds. The research was supported by the Brno University of Technology, Faculty of Civil Engineering –Specific Research No., FAST-S-24-8620 and FAST-S-25-8727. Special thanks to Mendel University in Brno and Masaryk University in Brno for their cooperation.

AUTHORS' ADDRESSES

Ing. Slávka Pobucká
Ing. Pavel Kučírek
doc. Ing. Karel Šuhajda, Ph.D.
Ing. Jan Holešovský, Ph.D.
Faculty of Civil Engineering, Brno University of Technology
Veveří 331/95
602 00 Brno, Czech Republic
Slavka.Pobucka1@vutbr.cz
Pavel.Kucirek@vut.cz
karel.suhajda@vut.cz
jan.holesovsky@vut.cz